

The Influence of 3D Printing Parameters on the Mechanical Behavior of PLA

IOANA-CATALINA ENACHE¹, IOANA-MADALINA CRISTINA¹, OANA-ROXANA CHIVU², ILEANA MATES², ELENA IONITA¹, GABRIEL GEAMBASU¹

¹University Politehnica of Bucharest, Faculty of Aerospace Engineering, Department of Engineering Graphics and Industrial Design, 313 Splaiul Independentei, 060042, Bucharest, Romania

²University Politehnica of Bucharest Faculty of Industrial Engineering and Robotics, 313 Splaiul Independentei, 060042, Bucharest, Romania

Abstract: Additive technologies are continually evolving and are crucial in numerous industries, including medical, aerospace, and automotive, but they can also play an important role in the prototyping phase. Due to additive manufacturing, amateurs and enthusiasts can construct simple projects as well as large projects with specialized usage in specific applications. When it comes to complex pieces, traditional manufacturing technologies such as milling, chipping, drilling, and so on have specific constraints, often need even additional production processes to complete the item. All of these constraints can be solved with additive technologies. This work investigates Fused Deposit Modeling (FDM) printing of many specimens with varying properties in order to analyze PLA (Poly Lactic Acid) material behavior following tensile testing. The collected findings will be analyzed in order to determine the specimens with the most significant behavior according on the modified parameters.

Keywords: 3D printer, PLA, material behavior, parameters, tensile testing

1. Introduction

Additive Manufacturing (AM), commonly known as 3D printing or 'rapid prototyping,' is a direct, layer-by-layer manufacturing technique. It can be used for experimental quick prototyping of diverse parts and can even result in functional, ready-to-use parts [1].

AM is largely geared on producing customized parts on a small scale, whereas traditional manufacturing technologies are geared toward mass production. 3D printing in small quantities is also less expensive than traditional manufacturing technologies, which require costly tools and preparation procedures prior to production. The healthcare industry is one of the most promising markets for 3D personalized items [2]. We can find developments ranging from dental implants used in dentistry to prosthesis and a variety of medical devices [3,4]. Because the fit of customized items manufactured with traditional technologies required multiple post-processing procedures, currently with AM processes personalization is possible and may be achieved reasonably easily [5, 6].

Material extrusion (MEX) procedures fall under the area of additive manufacturing and are classified into four types based on the material being extruded: Fused Deposition Modeling (FDM), Fused Granulate Fabrication, Fused Pellet Fabrication, and Powder Melt Extrusion.

These technologies are the most well-known and popular on the market, with FDM being the most extensively utilized material extrusion process [7], owing to the broad variety of printers and materials available on the market, as well as the technology's accessibility and ease of use.

FDM is also the first MEX series process that was designed. Scott Crump invented FDM technology in 1988, and the following year, Scott Crump started Stratasys Inc. He patented FDM technique in 1992, and the majority of the company's goods were based on it [1]. Stratasys has developed a wide range of rapid prototyping tools and materials to fulfill the needs of various sectors.

*email: catalina.enache@upb.ro

For FDM technology, the filament is heated to a semi-liquid condition in a chamber using thermal energy before being pushed through a nozzle and forming a smaller diameter filament that solidifies immediately after extrusion along the set path (Figure 1). Once the material has been extruded, the nozzle is elevated on the Z-axis and the process begins again, with another layer of material being deposited [8].

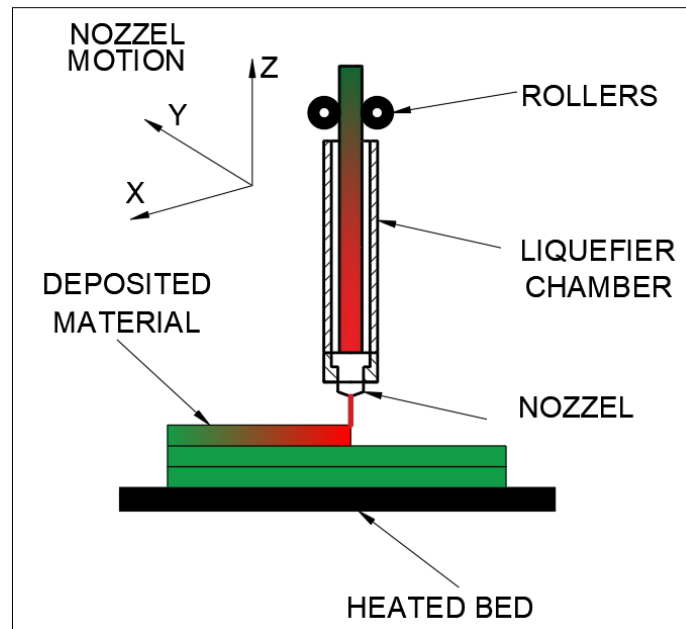


Figure 1. FDM process

A number of fundamental characteristics are shared by all extrusion-based processes, particularly [5]:

- Material loading (in the case of FDM, filament);
- Liquefaction of material
- Application of pressure to move material through the nozzle
- Extrusion
- Positioning the nozzle according to the X and Y axis trajectory
- Bonding the material to the previous layer
- Creating supports for complex structures

1.1. FDM technology's materials

PLA (polylactic acid), ABS (acrylonitrile-butadiene-styrene), nylon, TPU (thermoplastic polyurethane), PEEK (polyetheretherketone), ULTEM (polyetherimide), composites (e.g. PLA composites with carbon fiber), metals, and biodegradable materials are currently among the materials that can be used in FDM technology.

The printing of a prototype involves the selection of a specific material, which might be difficult due to the variety of alternatives. Simultaneously, with rapid prototyping evolution, there is concern about the effects of 3D printing on the environment. Researchers are beginning to focus greater attention on the negative impact of the carbon and waste footprint. To advance the concept of "green" material, biodegradable, recyclable, and compostable materials have been developed [8].

PLA is the most extensively used and representative material, and it can be processed on all FDM printers. It can be considered the most basic material for this technology because it exhibits low shrinkage when the molten material solidifies, this makes PLA very easy to use even for a beginner [9]. In contrast to most thermoplastic polymers, polylactic acid (PLA) is generated from renewable resources such as corn starch or sugar cane. The majority of plastics are derived from the distillation and

polymerization of nonrenewable oil deposits. 'Bioplastics' are plastics that are made from biomass. One of the most attractive things about this type of plastic is that it degrades naturally when exposed to the environment (in about 6-24 months) [8]. The tensile strength of multiple specimens made using FDM technology, with PLA as the material of choice, will be investigated. Conclusions about the mechanical behavior of these specimens will be formed based on changes in printing parameters such as printing speed, specimen filling method, and printing direction.

2. Materials and methods

The experimental investigation in this work is focused on 3D printing with PLA material.

The objectives of this work are:

- Modelling and 3D printing of specimens according to the proposed experimental design. The following process parameters are considered: material extrusion speed, filler pattern, degree of filling, and specimen orientation on the printing table.
- The influence of printing settings on the basic mechanical characteristics and structure of specimens is determined in order to acquire optimal printing specifications that maximize the mechanical properties of the material under examination.

2.1. Equipment used to determine mechanical properties

The Ultimaker 2+ 3D printer using a PolyTerra™ PLA filament was used for this work. The manufacturer's specifications for the 3D printer and mechanical properties of PLA are found in Table 1.

Table 1. The 3D printer's technical specifications [11]

Specifications	Values
Print sizes	223 x 220 x 205 (mm)
Filament diameter	2.85 mm
Extrusion	1 wire
Nozzle diameter	0.2/0.4/0.6/0.8(mm)
Deposited layer thickness	(0.06-0.6) mm depending on the nozzle used
Printing temperature	(180-260) C°
Print bed heating	(20-110) C°
Compatible material	ABS, PLA, TPU, PP, Nylon, CPE
File format	STL, OBJ, DAE
Software	Cura
Parameter	Value
Filament diameter	2.85 mm
Filament tensile strength	37MPa
Filament elongation	6%
Filament modulus of elasticity	4GPa
Filament density	1.3g/cm ³
Filament melting point	151°C
Filament glass transition temperature	62°C
Density	1.31g/cm ³ at 23°C
Melt index	14-20 g/10min
Melting temperature	162.6°C
Glass transition temperature	60.6°C
Molecular weight	66.000g/mol

The mechanical tests to determine the characteristic curves were carried out on the INSTRON 5982 testing machine. It is a static mechanical testing facility using BluHill Universal software. It is provided with two force cells (10 and 100 kN, respectively) and characteristics (Table 2) conforming to ASTM and ISO international standards (tensile, compression, bending, shear, and other applications) for testing plastics, composites, ceramics, and/or metals. [12]. This installation is equipped with a climatic chamber offering the possibility of testing in the temperature range of -70 to +250°C and a video extensometer Advanced Video Extensometer (AVE) with a 200 mm field of view.

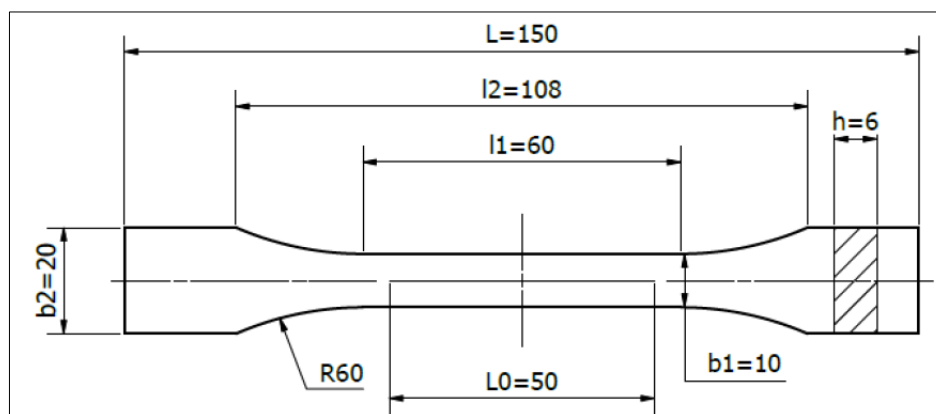
Table 2. INSTRON 5982 testing machine features [12]

Specifications	Values
Maximum speed	1016 mm/min
Minimum speed	0.0001 mm/min
Maximum force at maximum speed	100kN
Atmosphere	Designed for use under normal laboratory conditions

2.2. Design and modeling of 3D printed specimens

The design of the specimens was carried out according to the test standard for plastics, i.e. ISO 527 1 - "Determination of tensile properties of plastics. General principles" [13]. The ISO 527 2 standard was followed during the tensile test - "Determination of tensile properties of plastics. Test conditions for plastics manufactured by extrusion and melting" [14].

The modeling of the specimen (Figure 2) was carried out according to the mentioned standard using Inventor software.

**Figure 2.** Specimen dimension mm

2.3. Printing process

The simulation of the printing process leads to the choice of different printing parameters and to the NC code used for the actual printing.

The following parameters were considered for this work:

- The degree of filling (infill density) has a direct influence on the mechanical qualities of the printed parts; hence a lower filling degree reduces the mechanical properties of the parts.

- The pattern of filling also effects the mechanical properties of the printed portions, and may not withstand as well as the outside area - the walls of the printed pattern, because the walls have a 100% filling degree.

- Specimen orientation. Most of the time, the pattern is printed on the side, with no pockets or other elements that may disrupt the design's structure [1]. Vertically printed features have the worst mechanical properties, while specimen edge orientation has the greatest. In the case of edge-printed specimens, the wires are oriented parallel to the direction of loading, thus achieving samples with high mechanical strength. For the vertical orientation of the specimen, the layers are deposited perpendicular to the direction of stress (tensile, bending), thus facilitating much faster detachment of the layers [10].



- Printing speed. Too fast printing speeds can cause thread distortion because when a layer is produced, the previously deposited thread does not harden entirely by the time a new thread is deposited. As a result, the wires will deform due to the weight and voids particular to the pattern of filling [10].

The following parameters were chosen in order to determine which combination of characteristics is optimal: printing speed, degree of filling of the specimens, pattern of filling and orientation on the printing bed. For the infill density degree, a value of 70 and 40% was chosen, for the filling patterns triangular and tri-hexagonal patterns with the same composition were chosen, and for the printing speed

a value of 60 mm/s and 40 mm/s was chosen. As for the orientation on the printing bed, it was chosen on the plane and on the edge of the specimen.

Table 3 shows the parameters used to determine the optimal printing characteristics.

Table 3. Parameters used

Parameter	Characteristic	
	40	60
Printing speed [mm/s]	40	60
Filling patterns	Triangle	Tri-hexagon
Infill density %	40	70
Orientation on the printing bed	On plan 	On the edge 

A total of 18 specimens were printed, two for each parameter change, and coded according to Table 4, where the first number represents the infill density, followed by the letter "T" or "H" for the mode of filling, and at the end of the code is the printing speed used.

Table 4. Test specimen coding

Code	Infill density	Filling mode	Print speed	Orientation
70T60(_1,_2)	70%	Triangle	60 mm/s	On plan
70H60(_1,_2)	70%	Tri-hexagon	60 mm/s	On plan
70T40(_1,_2)	70%	Triangle	40 mm/s	On plan
70H40(_1,_2)	70%	Tri-hexagon	40 mm/s	On plan
40T60(_1,_2)	40%	Triangle	60 mm/s	On plan
40H60(_1,_2)	40%	Tri-hexagon	60 mm/s	On plan
40T40(_1,_2)	40%	Triangle	40 mm/s	On plan
40H40(_1,_2)	40%	Tri-hexagon	40 mm/s	On plan
L40T60(_1,_2)	40%	Triangle	60 mm/s	On the edge

The mechanical properties of specimens obtained using FDM technology depend on the selection of process parameters. The following printing parameters were specified for all specimens: layer height 0.2, a number of 2 outer walls, a number of 3 outer layers (linear deposition), distance between material deposition 3 mm, deposited layer thickness 0.8 mm, extrusion layer width 0.4 mm, nozzle diameter 0.4, printing temperature 200°C, working bed temperature 60°C. The specimens were printed one at a time to avoid problems that may occur during cooling of the material.

Figure 3 shows the printing simulation for the triangle filling pattern with 40% and 70% filling.

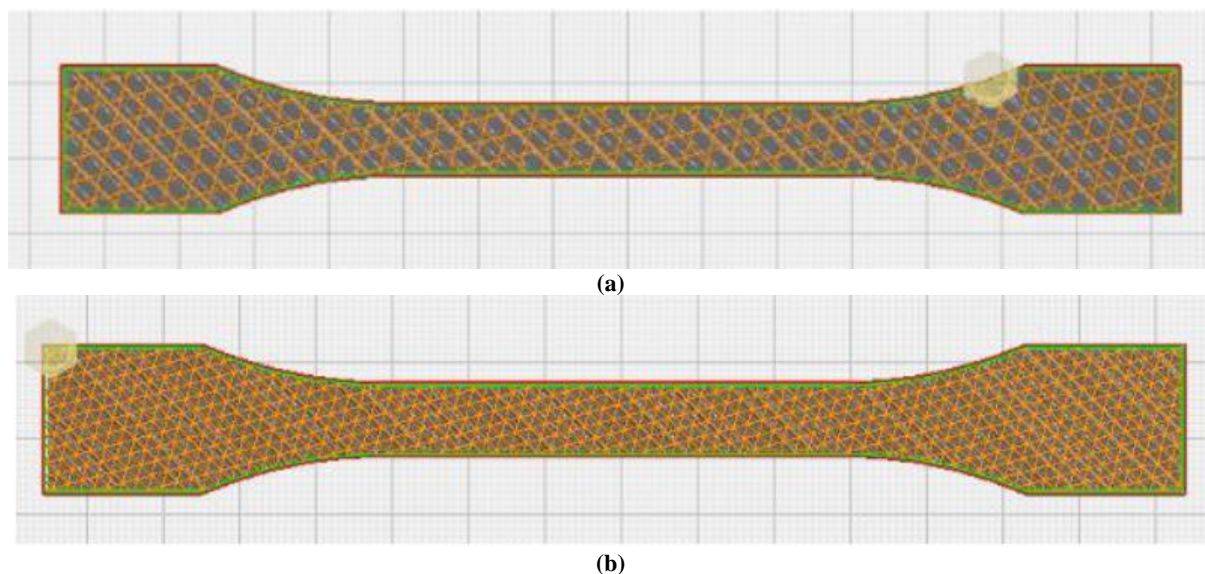


Figure 3. Different infill densities (a) Infill density 40% Triangles, (b) Infill density 70% Triangles

Uniaxial tensile tests were carried out on 3D printed specimens with different infill densities (40% and 70%). Two specimens were used for each degree of filling, which allowed the calculation of the mean and dispersion of the results.

For the L40T60(_1,_2) edge-printed specimens, parameters from the 40T60(_1,_2) code were applied: 60 mm/s speed, triangle fill, and 40% infill densities. Tree supports were used due to specimen orientation Figure 4. Post-processing involved removing supports with pliers. Two unmarked white dots were added to each specimen for elongation measurement per ISO 527, vital for the INSTRON testing machine's visual extensometer.

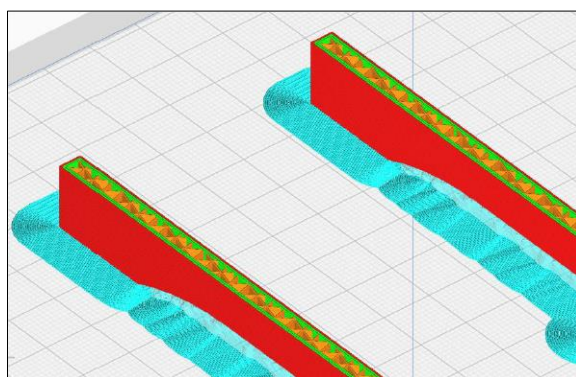


Figure 4. Simulation of the edge printing process



Figure 5. Experiment specimens

The tensile test was conducted using an INSTRON 5982 test machine with BlueHill software. Measurements included elongation at break, Young's modulus, yield strength, and force at break, with standard deviation and mean absolute deviation calculated for each set of specimens. The process involved:

Marking each specimen with an initial length of 50 mm using a spacer.

Measuring width and thickness at the narrow area and entering data into BlueHill software.

Fixing the specimen with clamping devices and running the machine until breakage, with results automatically calculated.

Test parameters included a 10 N force cell, preload speed of 2 mm/min, and test speed of 5 mm/min.

3. Results and discussions

The crack occurred outside length L_0 in 7 of the 18 printed examples, whereas the remaining 9 specimens ruptured in the stated area. Figure 6 shows the specimens after the tensile test. The specimens that ruptured outside the rupture zone are shown on the left side of the picture, followed by the other specimens. Analysis of the results shows that most of the specimens without a crack in the indicated area have a lower infill densities, i.e. 40%, and the first two specimens found in Figure 6 are those printed on the edge. There are many causes of out-of-area breakage. The main factor being the anisotropy of the

material, the plastic being extruded does not always retain the same layer thickness, again the infill densities is not 100%.

Another factor that can lead to out-of-area tearing is the printing method. If the printing has certain problems, for example nozzle retraction, or other problems related to the printing process of the specimen itself, an area inside the specimen may be created that is not as dense, or has certain voids, then it is normal for the crack to occur in that area.

Human errors also lead to cracks. If when the specimen is clamped between the two holders, it is not properly placed, or not tight enough by the clamping arms.



Figure 6. Specimens after testing

Figures 7, 8 show the characteristic curves of the specimens tested two by two for 40H40(_1,_2) and 40H60(_1,_2).

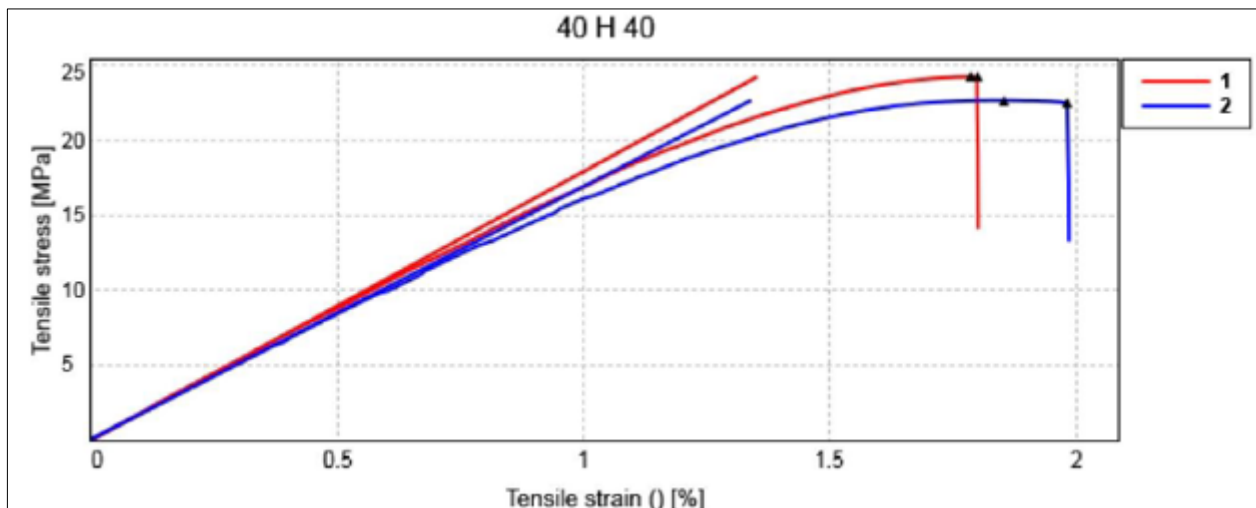


Figure 7. Characteristic curve of tested specimens (40%, tri-hexagon, 40mm/s)

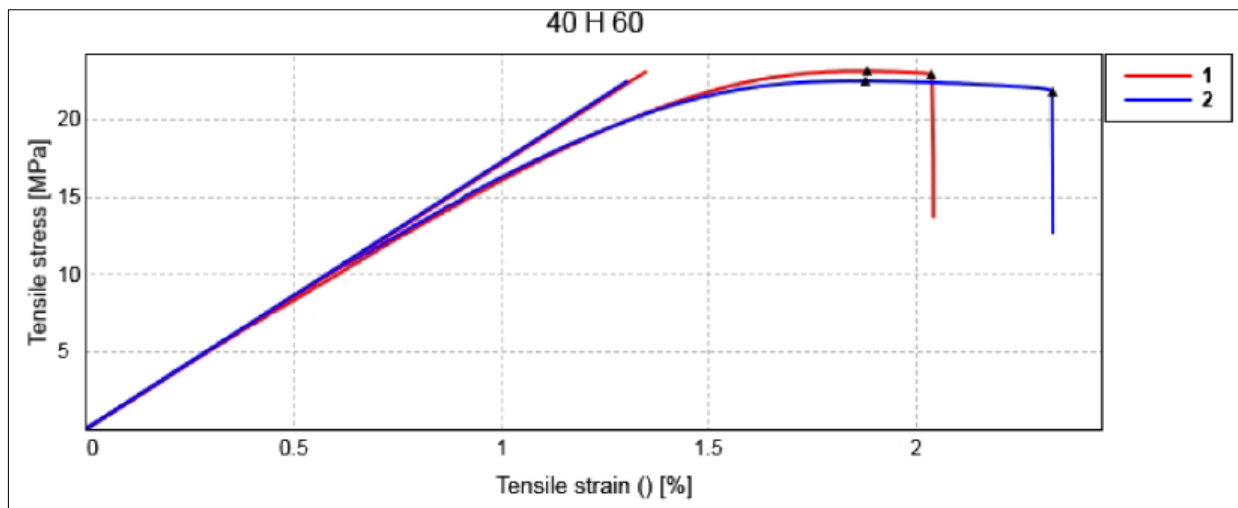


Figure 8. Characteristic curve of tested specimens (40%, trihexagon, 60mm/s)

Following the tests, the mechanical properties were determined, i.e. longitudinal modulus of elasticity, yield strength and elongation.

Table 5 shows the values for each individual specimen and the average value of the longitudinal modulus of elasticity/Young's modulus. Tables 6 to 8 show the mean values for elongation at break, resistance at break and force applied at break.

Table 5 Elasticity modulus values

Sample	Longitudinal modulus of elasticity [GPa]	Mean longitudinal modulus of elasticity [GPa]	Standard deviation
40H40_1	1.80	1.74	0.07
40H40_2	1.69		
40H60_1	1.72	1.72	0.01
40H60_2	1.73		
70H40_1	2.15	2.10	0.07
70H40_2	2.05		
70H60_1	2.11	2.15	0.06
70H60_2	2.19		
40T40_1	1.71	1.70	0.01
40T40_2	1.70		
40T60_1	1.78	1.76	0.03
40T60_2	1.73		
70T40_1	2.07	2.09	0.02
70T40_2	2.10		
70T60_1	2.12	2.10	0.03
70T60_2	2.09		
L40T60_1	2.27	2.27	0
L40T60_2	2.28		

Table 6. Values of elongation at break

Sample	Elongation at break [%]	Mean elongation at break [%]	Standard deviation
40H40_1	1.79	1.82	0.05
40H40_2	1.85		
40H60_1	1.88	1.88	0
40H60_2	1.88		
70H40_1	1.93	1.96	0.04
70H40_2	1.98		
70H60_1	1.90	1.89	0.01
70H60_2	1.88		
40T40_1	1.91	1.87	0.06
40T40_2	1.83		
40T60_1	1.78	1.77	0.01



40T60_2	1.76		
70T40_1	1.86	1.85	0
70T40_2	1.85		
70T60_1	1.69	1.75	0.10
70T60_2	1.82		
L40T60_1	1.47	1.46	0.01
L40T60_2	1.45		

Table 7. Breakage limit values

Sample	Breaking strength [MPa]	Mean limit of breaking [MPa]	Standard deviation
40H40_1	24.25	23.46	1.11
40H40_2	22.68		
40H60_1	23.13	22.82	0.45
40H60_2	22.50		
70H40_1	27.79	27.35	0.61
70H40_2	26.92		
70H60_1	27.20	27.91	1
70H60_2	28.62		
40T40_1	23.69	23.13	0.78
40T40_2	22.58		
40T60_1	22.57	22.51	0.08
40T60_2	22.45		
70T40_1	28.63	28.46	0.25
70T40_2	28.28		
70T60_1	26.72	26.78	0.08
70T60_2	26.84		
L40T60_1	25.80	26.00	0.01
L40T60_2	26.19		

Table 8. Force values applied at the time of breakage

Sample	Force applied at the moment of breakage [kN]	Mean force [kN]	Standard deviation
40H40_1	1.20	1.18	0.08
40H40_2	1.16		
40H60_1	1.18	1.17	0.02
40H60_2	1.15		
70H40_1	1.43	1.42	0.01
70H40_2	1.41		
70H60_1	1.42	1.42	0
70H60_2	1.42		
40T40_1	1.23	1.20	0.04
40T40_2	1.18		
40T60_1	1.15	1.15	0.01
40T60_2	1.16		
70T40_1	1.48	1.47	0.02
70T40_2	1.46		
70T60_1	1.37	1.39	0.03
70T60_2	1.41		
L40T60_1	1.32	1.33	0.01
L40T60_2	1.34		

Following the conducted study, we observed that:

- For specimens with a infill densities of 70% the maximum value of the elongated modulus of elasticity and the breaking limit is reached when it is printed at a speed of 60 mm/s.
- For 70% infill densities specimens the minimum value of the modulus of elasticity and the modulus of rupture is reached when it is printed at a speed of 40 mm/s.
- For 40% infill densities specimens the value of the longitudinal modulus of elasticity is equal for both speeds and the maximum value of the breaking limit is reached when printing speed is 40 mm/s.
- For specimens with a infill densities of 40% the minimum value of the breaking limit is obtained at a speed of 60 mm/s.

- For 70% infill densities specimens the maximum elongation at break is reached when printing speed is 40 mm/s.
- For 70% infill densities specimens the minimum elongation at break is reached when printing speed is 60 mm/s.
- For 40% infill densities specimens the maximum value of elongation at break cannot be estimated, due to the fact that both speeds have different results for tri-hexagonal and triangle filled specimens.
- For specimens with 70% trihexagonal infill densities, the maximum modulus of elasticity is reached when printing speed is 60 mm/s.
- For specimens with 70% trihexagonal infill densities, the minimum modulus of elasticity is reached when printing speed is 40 mm/s.
- For specimens with 70% triangle infill densities, the maximum modulus of elasticity is reached when printing speed is 60 mm/s.
- For specimens with 70% triangle infill densities, the minimum modulus of elasticity is reached when printing speed is 40 mm/s.
- For specimens with 40% trihexagonal infill densities, the modulus of elasticity value is equal regardless of printing speed.
- For specimens with 40% triangle infill densities, the maximum modulus of elasticity is reached when printing speed is 60 mm/s
- For specimens with 40% triangle infill densities, the minimum modulus of elasticity is reached when printing speed is 40 mm/s.

4. Conclusions

Additive technologies are emerging technologies that are very essential in many industries because, as demonstrated by their many uses, they may reduce manufacturing time but also prices. It has been shown that interest in this kind of technology is growing because of the benefits such as lighter weight of the parts, and at the same time the material can demonstrate high strength. This paper aims to highlight that the parameters and method by which printing is carried out are very important and can affect the prototype or the product.

Tensile testing of a number of 18 specimens printed with different parameters is performed to determine which combination of parameters has the highest degree of strength.

From the tests it was deduced that the tri-hexagon filler has a higher modulus of elasticity value than using a triangle filler. Also, the average values of the elongation at break are generally higher than for the triangle filler. However, the tensile strength value is at its maximum when using the triangle filler.

Acknowledgments: This work was supported by a grant from the National Program for Research of the National Association of Technical Universities - GNAC ARUT 2023.

References

1. CHUA, C.K., LEONG, K.F., *3D Printing and Additive Manufacturing Principles and Application The 5th edition of Rapid: Prototyping Principles and Application*. World Scientific Publishing, Singapore, 2017, 23-30.
2. ULMEANU, M.E., DOICIN, C., BĂILĂ, D., BĂILĂ, I., RENNIE, A., NEAGU, C., LAHA, S., Comparative Evaluation of Optimum Additive Manufacturing Technology to Fabricate Bespoke Medical Prototypes of Composite Materials, *Mater. Plast.*, **52**(3), 2015, 416-422.
3. RADUICA, F.-F., SIMION, I., IONITA, E., A Study on Parametric Design of Line Tendon Based Prosthetic Finger Using Programming Techniques, *Journal of Industrial Design and Engineering Graphics*, **16** (2), 2021, 4-10.
4. FAROOQ, H. MUSTAFA, M., FAKHRI, A., A Systematic Review of Partial Hand Prostheses, *Global Scientific Journal of Biology*, **8** (1), 2023, 82-98,



5. CHUA, C. K., WONG, C. H., YEONG, W. Y., Standards, Quality, Control, And Measurement Sciences In 3D Printing and Additive Manufacturing. Academic Press, An imprint of Elsevier. Singapore, 2017, 159-179.
6. BELGIU, G., TURC, C., CARAUSU, C., Selection of Subtractive Manufacturing Technology Versus Additive Manufacturing Technology for Rapid Prototyping of a Polymeric Product, *Mater. Plast.*, **57**(4), 2020, 343-352.
7. GIBSON, I., ROSEN, D., STUCKER, B., *Additive Manufacturing Technologies: 3D Printing, Rapid Prototyping, and Direct Digital Manufacturing - second edition*, Springer-Verlag Publishing. New York, 2015, 30-34.
8. HERRERA-PONCE DE LEÓN, E., ALEXANDER, U. PÉREZ, V., KHAN, Z.N., HAUSER C.A.E., Intelligent and smart biomaterials for sustainable 3D printing applications, *Current Opinion in Biomedical Engineering*, **26**, 2023, 100450, ISSN 2468-4511, <https://doi.org/10.1016/j.cobme.2023.100450>.
9. ANTIĆ, J., MIŠKOVIĆ, Ž., MITROVIĆ, R., STAMENIĆ, Z., ANTELJ, J., The Risk Assessment of 3D Printing FDM Technology, *Procedia Structural Integrity*, **48**, 2023, 274-279, ISSN 2452-3216, <https://doi.org/10.1016/j.prostr.2023.07.132>.
10. MAZURCHEVICI, A. D., CARAUSU, C., CIOFU, C., POPA, R., MAZURCHEVICI, S.-N., NEDELICU, D., Infill and type influence on tensile strength of PLA biodegradable material using FDM technology, *International Journal of Modern Manufacturing Technologies*, **11** (2), 2019, 44-49, ISSN 2067-3604.
11. ***<https://ultimaker.com/3d-printers/s-series/ultimaker-2-connect/> (accessed on 11.08.2023)
12. ***<https://www.instron.com/en/products/testing-systems/universal-testing-systems/high-force-universal-testing-systems/5989-floor-model> (accessed on 11.08.2023)
13. *** ISO 527 – Determinarea proprietăților de tracțiune a materialelor plastice - Condiții de testare pentru materiale plastice fabricate prin extrudare și topire, 2012
14. *** <https://www.iso.org/standard/56046.html> (accessed on 28.05.2023)

Manuscript received: 24.08.2023